

APPENDICES

[Appendix A: Table Showing the Steepness of Forage Fish](#)

[Appendix B: Further Elaboration on Functional Responses](#)

[Appendix C: Figures from Case Studies in Chapter 4](#)

[Appendix D: Equations and Further Descriptions for Ecopath Analysis](#)

[Appendix E: Supplementary Figures and Tables for Ecopath and EwE Analysis](#)

[Appendix F: EwE Model Descriptions](#)

[Appendix G: EwE Management Strategy Evaluation \(MSE\) Module](#)

[Appendix H: A Synthesis of the Joint Effects of Depletion of Forage Fish Biomass and Predator Diet Dependency \(The PREP Equation\)](#)

APPENDIX A: Steepness of Forage Fish

Species name	n							Ricker Steepness		Bev-Holt Steepness	
		log.alp ha	se.log.al pha	var. log. alpha	alph a	small. m	large. m	Low estimate of M	High estimate of M	Low estimate of M	High estimate of M
Anchovy (<i>Engraulis encrasiculus</i>)	2	0.7	0.13	0	2.01	0.8	1.2	0.418	0.302	0.386	0.295
Atlantic herring (<i>Clupea harengus</i>)	18	0.73	0.28	1.31	2.08	0.1	0.19	2.267	1.357	0.839	0.732
Atlantic mackerel (<i>Scomber scombrus</i>)	2	1.11	0.91	1.29	3.03	0.18	0.2	1.914	1.759	0.808	0.791
Atlantic menhaden (<i>Brevoortia tyrannus</i>)	1	2.2	0.12		9.03	0.37	0.64	2.576	1.662	0.859	0.779
Gold-spotted grenadier anchovy (<i>Collia dussumieri</i>)	1	2.73	0.19		15.3 3	1.3	2.02	1.44	1.012	0.747	0.655
Gulf menhaden (<i>Brevoortia partonus</i>)	1	1.25	0.16		3.49	0.8	1.1	0.65	0.504	0.522	0.442
Horse mackerel (<i>Trachurus rachurus</i>)	2	0.52	0.8	0	1.68	0.15	0.48	1.382	0.545	0.737	0.467
Northern anchovy (<i>Engraulis mordax</i>)	1	0.33	0.41		1.39	0.4	1.31	0.542	0.21	0.465	0.21
Pacific sardine (<i>Sardinops sagax</i>)	2	0.66	0.89	1.56	1.93	0.4	0.8	0.704	0.405	0.547	0.376
Spanish sardine (<i>Sardina pilchardus</i>)	1	-0.56	0.75		0.57	0.33	0.33	0.31	0.31	0.302	0.302
Sprat (<i>Sprattus sprattus</i>)	3	0.87	0.55	0.71	2.39	0.33	1	0.975	0.402	0.644	0.374

Source: A.O. Shelton.

APPENDIX B: Further Elaboration on Functional Responses

Predator Functional Relationships

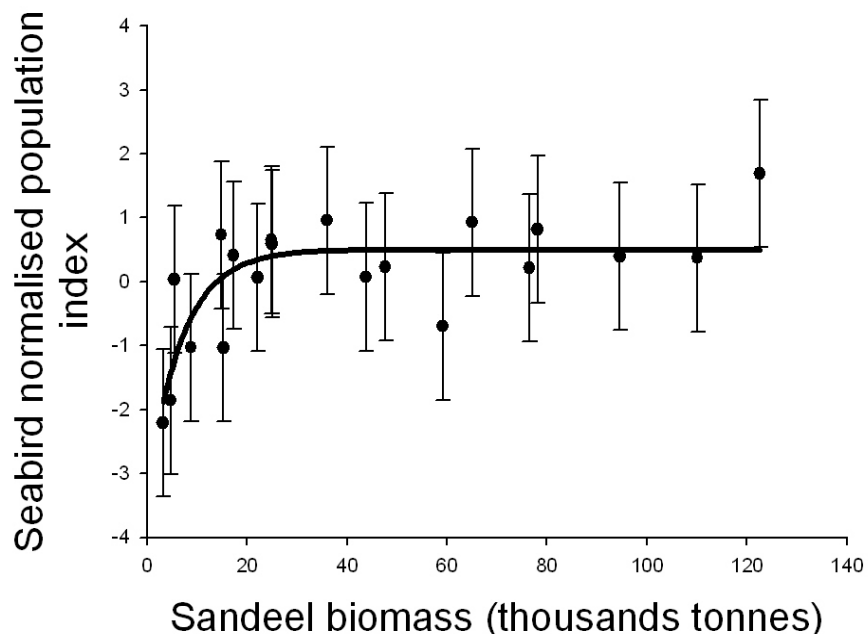
There is a strong theoretical basis indicating a relationship between indices of foraging success in marine predators and the state of their food supply, especially for forage fish (Cairns 1987). Holling (1959) described three types of functional responses in the feeding rate of predators to prey density: Type I is linear over a specified range of prey density; Type II is a hyperbola that reaches an asymptote; and Type III is a sigmoid function that accelerates initially, followed by decelerating prey consumption, and that also approaches an asymptote as the density of prey increases.

A more general representation of these types of responses can be found in the relationships between food density (or total biomass) and variables that are a consequence of changes in the rate of feeding, such as reproductive and survival rates, growth rate or changes in the size of breeding populations. Most often, especially for marine predators, feeding cannot be measured directly and it is easiest to measure one of these variables instead. Another advantage is that the variable being measured can be a better indicator of relative fitness than feeding rate.

As for the functional response, this relationship (herein referred to as a functional relationship) between forage fish density or population size and the response of a predator like a seabird or a marine mammal will have a particular functional form when measured on an annual time scale. In practice, predator responses can be represented as a number of measurements that correlate with fitness, such as breeding population size, breeding success rate, offspring growth rate, and foraging trip duration (Boyd and Murray 2001, Piatt *et al.* 2007). In theory, we would expect the functional form of this relationship to be sigmoid or hyperbolic-asymptotic (comparable with the Type II or Type III functional responses described by Holling, 1959). An example is shown in Figure B1 and there is increasing empirical support for the existence of these types of relationships between predator responses and prey population size or density (e.g., Boyd and Murray 2001, Furness 2002, Piatt *et al.* 2010, Field *et al.* 2010).

Figure B1

Functional Relationship Between Annual Seabird Breeding Population and the Abundance of Sand Eels in the Shetland Islands of the North Sea: 1986–2006.

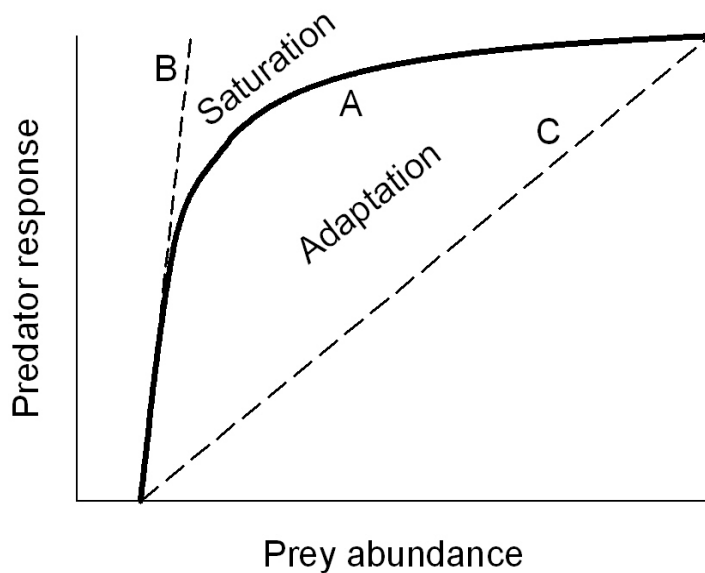


The normalized population index, shown as a mean \pm SE, included four seabird species (Common murres *Uria aalge*, Razorbill *Alca torda*, black-legged kittiwake *Rissa tridactyla*, Arctic tern *Sterna paradisaea*) from the database of the Joint Nature Conservation Committee (JNCC <http://www.jncc.gov.uk/smp/>) and applies a procedure for normalizing and combining the individual population indices developed by De la Mare and Constable (2000) and applied by Boyd and Murray (2001). This is a development of the relationships examined by Furness (2002).

The asymptotic form of the relationship derives from two processes involving either “saturation” or “adaptation” of the predator response (Fig. B2). In the case of saturation, there will be an upper limit to the ability of highly K-selected (i.e., have few offspring) predators such as seabirds to produce offspring and also for predator populations to grow in response to transient high food densities. This leads to saturation of the capacity of predators to respond to high food availability and a change in the response from the line labeled B towards the line labeled A in Figure B2. It is also a response that is closest to the original concept of function responses as defined by Holling (1959). Alternatively, the response of predators to declining food availability may be to adopt different foraging strategies depending upon prey density and this would lead to an asymptotic functional relationship due to predator behavioral buffering. This has been shown to be an important mechanism producing a non-linear functional relationship between Antarctic fur seals (*Arctocephalus gazella*) and their main prey species, Antarctic krill (*Euphausia superba*) (Mori and Boyd 2004). This effect is illustrated by the difference between lines A and C in Figure B2. Here, line C illustrates the theoretical functional response if the foraging strategy used when prey density is high is also used throughout the range of variation in prey density. Behavioral adaptation can elevate the response but predators will eventually run out of options for behavioral adaptation, as illustrated by curve A of Figure B2, and this leads to a rapid decline in the predator response index.

Figure B2

Diagrammatic Representation of the Functional Relationship Between a Marine Predator and the Abundance of a Forage Fish Species (Line A).



Line B shows an alternative response under circumstances when saturation of the predator response does not occur. Line C represents a response when there is no adaptation of foraging behavior to maintain high foraging success even when prey abundance declines.

In most cases when predator responses are observed (e.g., Piatt *et al.* 2007) it is impossible to know which of these two mechanisms is operating. However, it is most probable that both the shape of the functional relationship and the mechanism that

is most important in any particular example will depend on which type of variable is used to represent the predator response. Piatt *et al.* (2007) provided several illustrations of this for murres and black-legged kittiwakes.

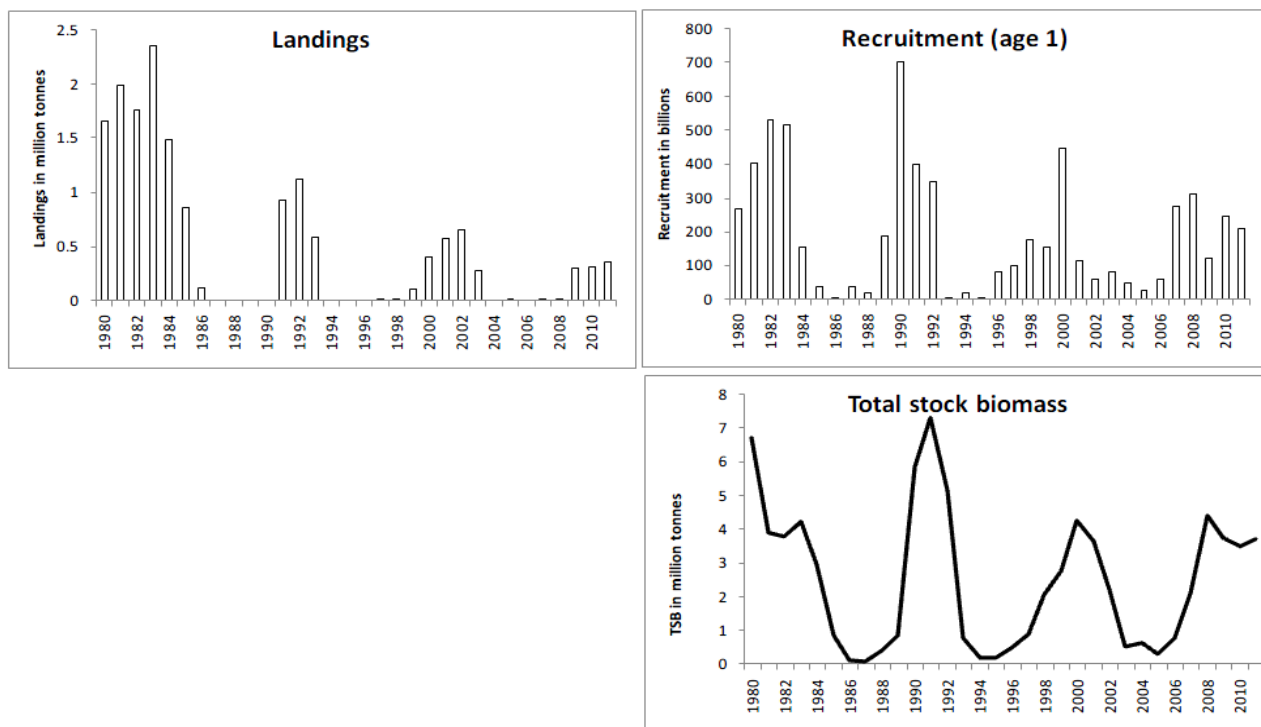
It becomes possible to create new approaches to the management of forage fish by using these types of relationships (Richerson *et al.* 2010). Predators often have considerable existence value and in many places where forage fish are harvested there is also legislation to protect and maintain populations of predators like seabirds and marine mammals. Consequently, knowledge of the functional relationship between predator responses and forage fish population size means that it should be possible to develop management strategies that help to maintain forage fish populations above the threshold at which rapid declines in predator responses are likely to occur (Fig. 3.2). Establishing harvest rules that use this approach could be the key to delivering the levels of fishing that minimize ecological impacts.

A feature of many of the functional relationships measured to date is the relatively low forage fish population size at which a steep decline in predator response is observed (e.g., Fig. B1) and the steepness of the decline thereafter. This may result in a situation when forage fish populations lie above the threshold most of the time (hence suggesting that fishing is possible), but it would be necessary to be very cautious about allowing fishing to drive the forage fish population below the threshold population size because of the extreme predator response that could be induced as a result. Additional care would also be needed in order to ensure that management of a fishery did not exacerbate the frequency of apparently natural events when forage fish populations dipped below the threshold at which predators began to show extreme reductions in performance. This could be possible even when using a harvest strategy that prevented fishing occurring at or below the threshold forage fish population size. Finally, while the reference in the present study has been to forage fish populations as a whole, it needs to be recognized that some predators, such as breeding seabirds and seals, are constrained in space and time so that a harvest strategy intended to minimize the probability of inducing a decline in predator populations using the kind of information about functional relationships illustrated in Figure B1 would also need to consider these factors.

APPENDIX C: Case Study Figures

Figure C1

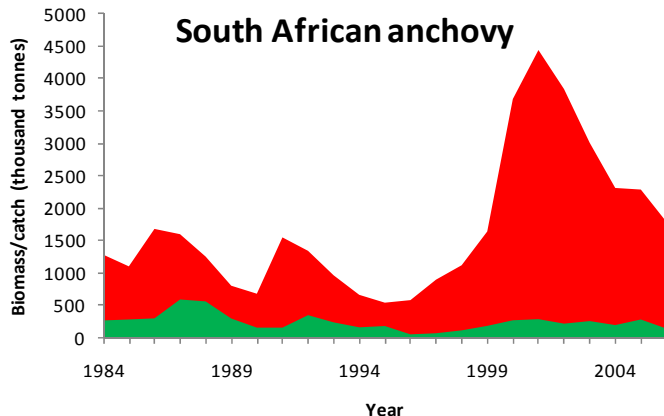
Barents Sea Capelin Landings (million tonnes), Age-1 Recruitment (millions), and Total Stock Biomass (million tonnes).



Source: ICES 2011.

Figure C2

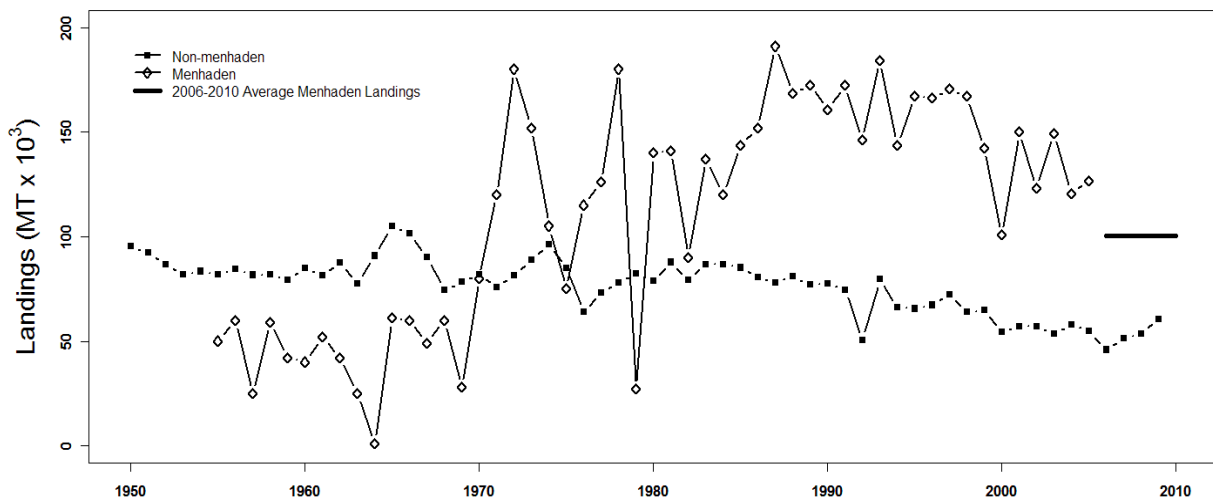
Changes in South African Anchovy Recruit Biomass from Survey Estimates (Red) and Total Catches (Green).



Source: de Moor *et al.* 2008.

Figure C3

Chesapeake Bay commercial Fisheries Landings, 1950 to Present.

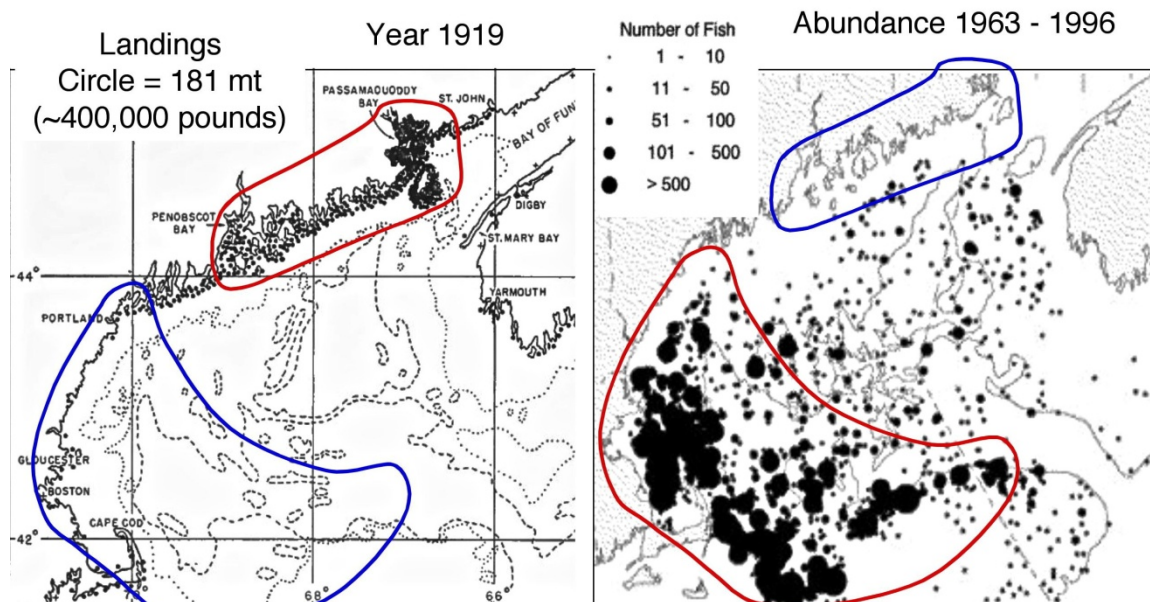


The non-menhaden landings are the aggregate commercial catch of all species included in NOAA-NMFS statistics. Menhaden catches specific to Chesapeake Bay were provided by NOAA-NMFS and ASMFC. Because statistics on purse-seine reduction fishery landings of menhaden are proprietary for recent years because a single company (Omega Protein) conducts the fishery,

only the mean purse-seine reduction landings from Chesapeake Bay for years 2006-2010 were available. The combined mean purse-seine reduction fishery landings and mean purse-seine bait landings of menhaden are depicted in the figure.

Figure C4
Herring Distributions in the Gulf of Maine and Georges Bank for 1919 and the Period from 1963 to 1996.

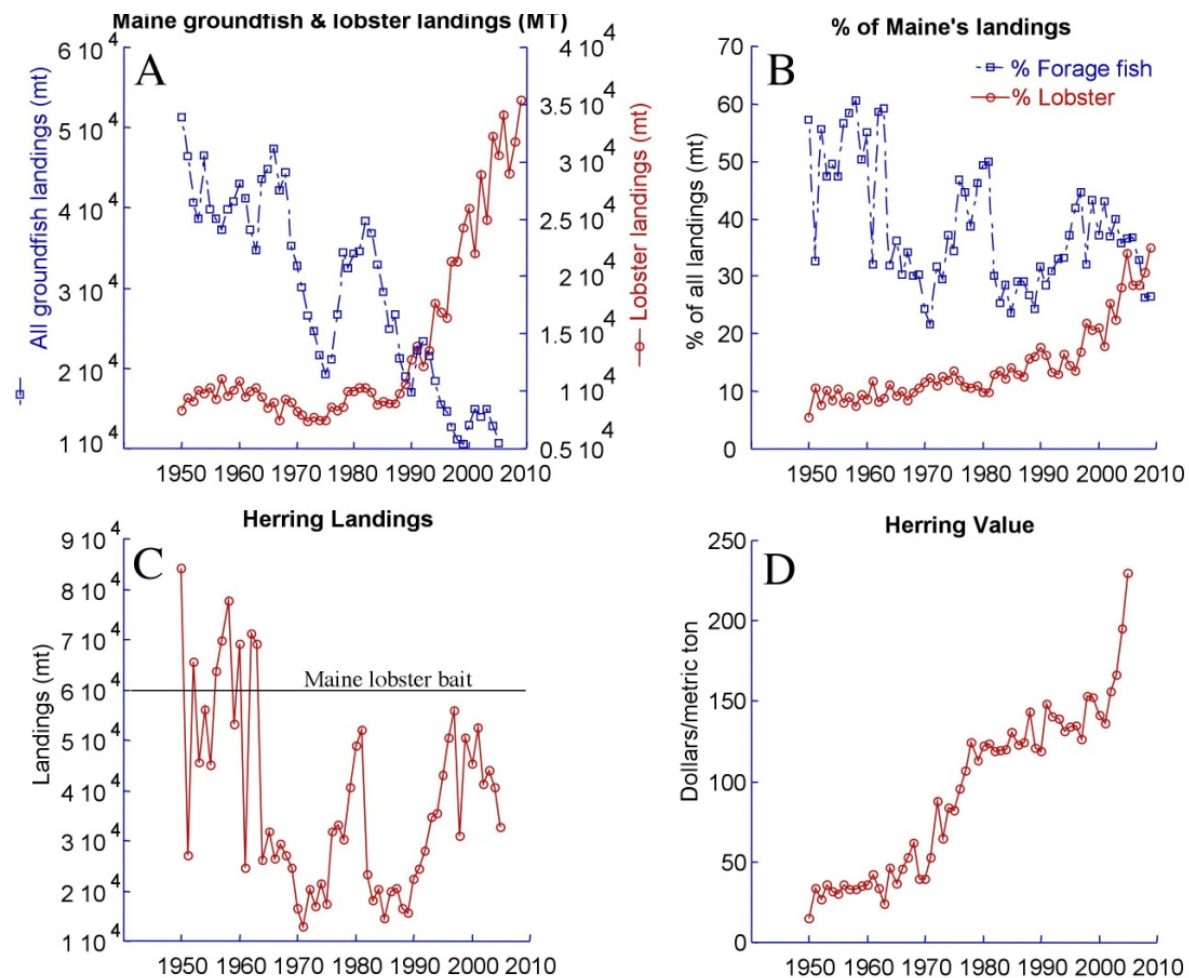
Herring Distribution and Abundance Gulf of Maine & Georges Bank



Herring hot-spots are in red and cold spots in blue. Note that the northeast hotspot and southwest cold spot in 1919 reversed in recent decades.

Figure C5

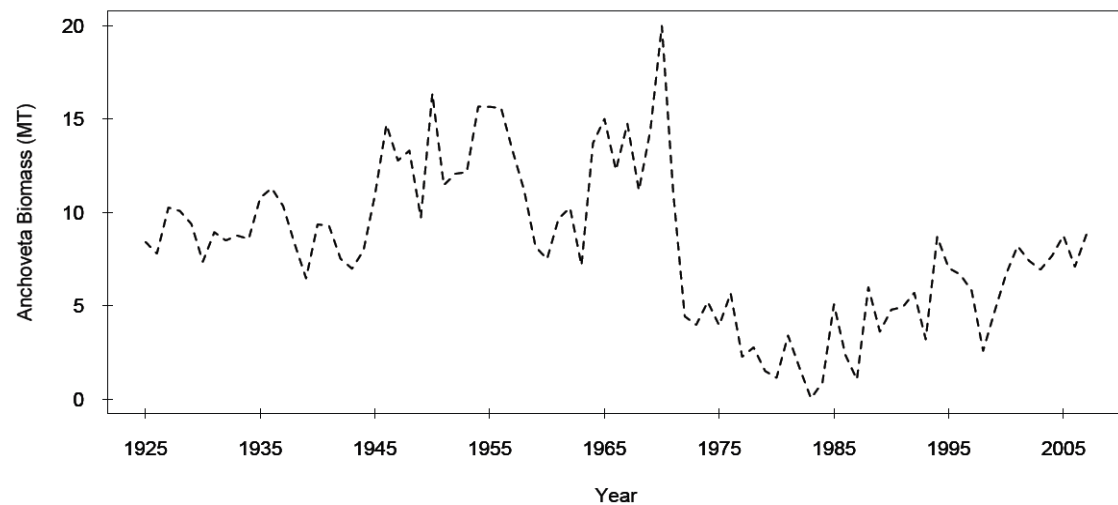
Fisheries Chronologies in Maine Driving the Herring Bait Industry.



A. Landings of groundfish and lobsters. B. Percent of Maine's fisheries landings in forage fishes (herring, alewife, blueback herring, and menhaden) and lobsters. C. Herring landings. (The horizontal line shows the amount of herring bait used in Maine in 2009.) D. Herring value since 1950. Source: Maine Department of Marine Resources, <http://www.maine.gov/dmr/commercialfishing/historicaldata.htm>.

Figure C6

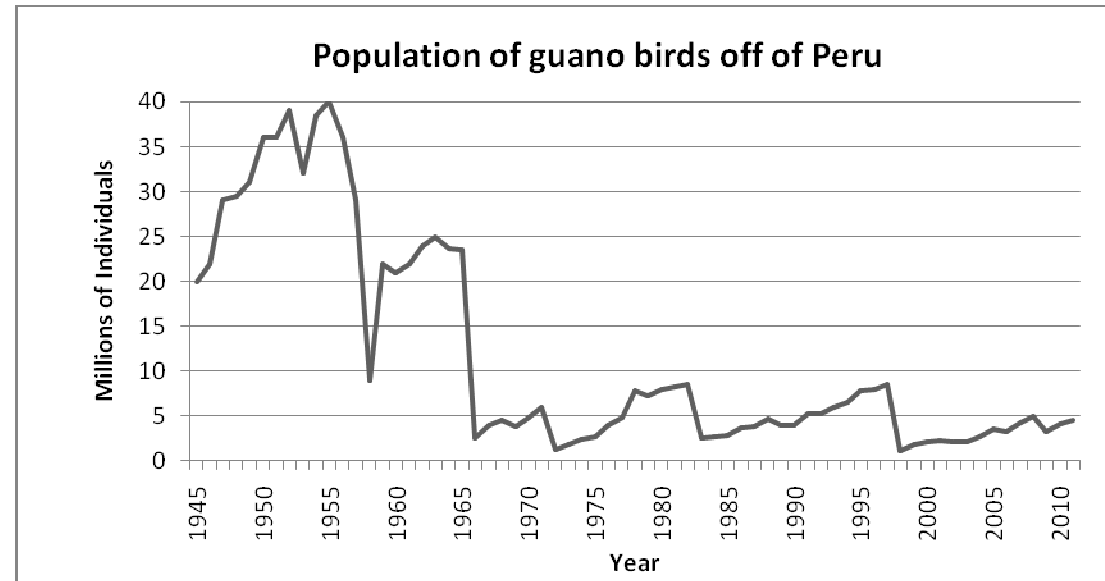
Biomass of the North and Central Stock of Peruvian Anchoveta (*Engraulis ringens*)



This graph is based on an empirical model (Jahncke *et al.* (2004; 1925-to mid-1950s); on Virtual Population Analysis to account for the fluctuating biomass of predators, and calibrated by hydro-acoustic estimates (Pauly and Palomares 1989; mid-1950s to mid-1980s) and on hydro-acoustic surveys conducted by Instituto del Mar del Perú (IMARPE) from the mid-1980s to the 2000s.

Figure C7

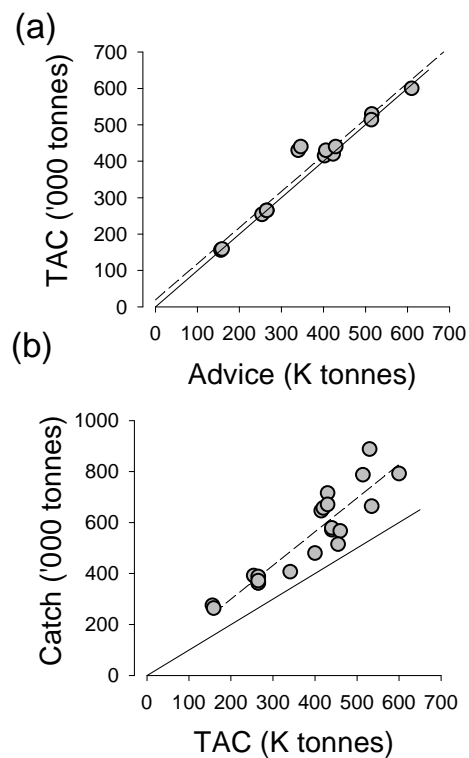
Population of Guano Birds (in millions) off the Peruvian Coast: 1945–2010



Guano birds are Guanay cormorant (*Phalacrocorax bougainvillii*), Peruvian booby (*Sula variegata*), and Peruvian pelican (*Pelecanus thagus*). An enormous decline was observed in 1966 when the guano bird population dropped to 2.5 million individuals from 23.5 million individuals in 1965. Source: AGRORURAL, personal communication.

Figure C8

The Annual TAC for North Sea Herring Plotted Against the Annual ICES Advice: 1987–present.



Graph (a) shows the annual TAC for North Sea herring plotted against the annual ICES advice; graph b represents the annual catch of North Sea herring plotted against the annual TAC. The estimated catch included discards. Each dot represents a different year. Fewer points are present in (a) because in several years the annual advice could not be presented as a predicted catch. The solid line in graph (b) illustrates the trajectory of the points if the management system had been followed perfectly from the preceding step in the sequence. The dashed line shows the actual relationship. Note that in (a) the lines lie so close to one another that it is difficult to see deviation. The distance of the dashed line from the solid line gives a relative measure of the faithfulness with which the ICES scientific advice is translated into a TAC (a) and the TAC is translated in to actual catch (b).

APPENDIX D: Equations and Further Descriptions for Ecopath Analysis

Equations

We estimated the portion of every predator's production supported by forage fish for all forage fish predators and across all ecosystem models using modified equations from Hunsicker *et al.* (2010). First, we calculated the total annual production (P_j , units: t/km²/yr) of every forage fish predator group j in every Ecopath model using Equation (D-1), in which predator group j 's biomass (B_j , units: t/km²), was multiplied by that respective predator group's production-to-biomass ratio (P/B , units: yr⁻¹). Second, we found the portion of each predator group's total annual production ($P_{i,j}$) supported by forage fish prey groups (i), by multiplying predator group j 's respective diet dependency on forage fish ($D_{i,j}$) by P_j using Equation (D-2). The total support service contribution of forage fish to ecosystem predator production (S_z) therefore can be found using Equation (D-3), as the product of ($D_{i,j}$) and (P_j) summed over all forage fish groups (i) and predator groups (j) in an ecosystem. Hunsicker *et al.* (2010) showed that $D_{i,j}$ is equivalent to the contribution of prey group i to predator group j 's production ($P_{i,j}$) when assimilation and energy content of prey items are roughly equivalent. In the absence of detailed data on these variables, we assume they are all equal to each other but presume that our analysis underestimates $P_{i,j}$, because of the generally high energy content of forage fish species compared to other predators. Thus, our estimates for the support service contribution of forage fish to ecosystem predator production can be considered conservative.

$$P_j = B_j \left(\frac{P}{B} \right)_j \quad \text{Eq. D-1}$$

$$P_{i,j} = D_{i,j} P_j \quad \text{Eq. D-2}$$

$$S_z = \sum_j \sum_i D_{i,j} P_j \quad \text{Eq. D-3}$$

We estimated the support service contributions of forage fish to the catch (S_C) and catch value (S_V) of other commercially targeted model groups by using equation (D-3), except that the predator group's total annual production (P_j) was replaced by the catch (C_j , equation (D-4) and catch value (V_j , equation D-5) of each predator group j .

$$S_C = \sum_j \sum_i D_{i,j} C_j \quad \text{Eq. D-4}$$

$$S_V = \sum_j \sum_i D_{i,j} V_j \quad \text{Eq. D-5}$$

Ecopath Model Requirements

For Ecopath models to be included in our analysis they needed to: (1) represent a marine or estuarine ecosystem within the last 40 years and (2) have all necessary data and parameters freely available. Furthermore, it was important that all data were collected from Ecopath models and not other modeling software. This ensured that differences between ecosystems were the result of the respective ecosystem parameters and not an artifact of the modeling framework.

Data Extraction and Analysis

We extracted catch data, diet composition matrices, biomass data, production-to-biomass ratios and total model area (km²) directly from Ecopath model publications and transferred them to Microsoft Excel spreadsheets. We used catch data estimates (landings + discards), since the majority of the Ecopath models contained catch data and not landings data alone. Several models only had landings data available with no estimates of discards, so we assumed that discards were zero for these ecosystems. We obtained data from Ecopath models used in this analysis from peer-reviewed publications, grey literature and theses. All catch data and biomass data that were not in units of (t/km²/yr) and (t/km²), respectively, were converted before being entered on spreadsheets. When Ecopath software files (.mdb) were available for a model, we verified the data with a corresponding publication before transferring it into spreadsheet form.

Ecopath models contain interactive "groups" which are comprised of one or more species. We created an inventory of all species (or the lowest taxonomic classification possible) for each of these model groups when this information was provided in model publications. The grouping of species into model groups is assigned by the model authors and for the purposes of this analysis cannot be changed. Since catch, diet matrix, and biomass data were compiled for each model group, it is not possible to determine the relative contributions of species within each model group. We assumed that as long as a single forage fish species was part of a model group, then that group should be considered as a forage fish group. For instance, if an anchovy species were a component of a model group called "Small Pelagics," along with gobies and juvenile mackerels, then this group would be

considered a forage fish group, even though gobies and juvenile mackerels do not meet our definition of forage fish. The one exception to this rule applies to krill forage fish (Order: Euphausiae), which are only contained as separate model groups in 9 of the 72 Ecopath models in this analysis¹. In the remaining Ecopath models where krill are present in the ecosystem, they are grouped into various "Zooplankton" groups. We chose to exclude these "Zooplankton" model groups as forage fish groups in this analysis and only included contributions of krill from models with defined krill model groups. We acknowledge that this modeling approach may cause differences between ecosystems in terms of forage fish contributions (i.e. those that have a separate krill group and those that do not) but assumed in this analysis that if model authors grouped krill separately it was due to their importance in the ecosystem. We found it most appropriate to include krill groups in this analysis when present rather than completely excluding them.

All 72 Ecopath models were used to calculate forage fish catch and the supportive contribution of forage fish to catch volume (t/km²/yr), while only 56 Ecopath models (Table E-1, Appendix E) could be used to calculate their respective monetary values (2006 USD/km²/yr).

Calculation of Ex-vessel Prices

We used a global ex-vessel price database developed by Sumaila *et al.* (2007) to obtain ex-vessel price data for all fished species in all participating countries in our Ecopath models. Ex-vessel price is defined as the real prices that fishermen receive for their products before processing. In this analysis we refer to "value" as ex-vessel real price times quantity (gross returns) and not the economic profit (net returns). We calculated a weighted average of ex-vessel price based on the share of the catch for all countries with fisheries in the respective Large Marine Ecosystem (LME) in which an Ecopath model was located. We obtained catch data for every country participating in fisheries in a respective LME in the year 2006 from the Sea Around Us project LME database (Watson *et al.* 2004; www.searroundus.org) in order to weight the respective contributions to catch by each country in an LME. LMEs are marine areas defined largely by similar geology, productivity, and water circulation (Sherman & Alexander 1986). For small geographic areas (e.g. estuaries, lagoons, and small coastal areas), we assumed that only the country surrounding these waters fished them. We made this assumption because detailed information about which specific countries fish within an Ecopath model area is not usually published. For example, we assumed the United States of America to be the only country fishing the Chesapeake estuary, even though the LME area in which it resides includes both the Unites States and Canada as the major fishing countries. For the few Ecopath models that were located outside of a defined LME area (e.g. Central North Pacific Ocean, Central Atlantic Ocean and Eastern Subtropical Pacific Ocean, we assumed participating fishing countries to be those nearest to, and surrounding the model locations. Lastly, we assumed Ecopath models of island countries and territories that fell outside of LME boundaries (e.g. the Azores Archipelago) to be fished only by that country or the country of which it is a territory.

We compiled country-specific ex-vessel real price data for every species in all 56 Ecopath models using an ex-vessel price database (Sumaila *et al.* 2007). To account for differences in prices between countries operating in a given LME, we calculated a weighted average based on the total catch of all participating countries within that LME. When model groups consisted of two or more species, the ex-vessel model group price was found by averaging the country-weighted ex-vessel prices for all respective species within that model group. We used these averaged ex-vessel model group prices to calculate fisheries value (2006 USD/km²/yr) for each respective model group in all 56 Ecopath models.

Latitude and Ecosystem Groupings

Ecopath models were grouped by latitude and by ecosystem type in this analysis. Latitude groupings consisted of three categories: Tropical-Subtropical (< 30° N – < 30° S), Temperate ($\geq 30^{\circ}$ N – 58° N and $\geq 30^{\circ}$ S – 58° S), and High latitude ($> 58^{\circ}$ N and $> 58^{\circ}$ S). Models were also grouped into general ecosystem-type categories to allow for other comparisons. These ecosystem types include: coastal upwelling ecosystems, semi-enclosed ecosystems, non-upwelling coastal ecosystems, tropical lagoon ecosystems, open ocean ecosystems, Arctic high latitude ecosystems, and Antarctic ecosystems. Models were only categorized into one ecosystem group and needed to meet specific criteria in order to be added (Table E-1, Appendix E).

¹ Ecosystem models which included a separate krill model group include; Antarctic Peninsula, Central Chile, Falkland Islands, Kerguelen EEZ, Northern California Current, North Sea, Hecate Straight - Northern British Columbia, South Orkneys / South Georgia region and Western Bering Sea.

Global Extrapolation

The Sea Around Us project has produced independent estimates of forage fish catch values by Economic Exclusive Zone (EEZ) and High Seas Area (HSA). In the Sea Around Us fisheries databases, the majority of forage fish species are grouped into two functional groups, "Herring-likes" and "Anchovies." We assumed that the total direct forage fish catch value estimated by the Sea Around Us for each respective EEZ and HSA was the sum of these two functional groups.² This is an underestimate of forage fish catch values as it does not include some forage fish species that are grouped into other functional groups. As the Sea Around Us does not provide its own estimate of the supportive value of forage fish to commercial fisheries, this needed to be extrapolated. This analysis provides the first estimates of the supportive values of forage fish to commercial fisheries, allowing for the results to be used to further estimate the total forage fisheries value (direct plus supportive) within each EEZ and HSA.

In our analysis, Ecopath models existed for 64 (25 percent) of the total 257 EEZs and HSAs. Ecopath models generally represented areas of historical importance to fisheries and/or scientific research (e.g., northern Humboldt Current and North Sea). In contrast, other areas such as the Indian Ocean or remote islands have almost no Ecopath model representation.

For each Ecopath model, we calculated an Ecopath value ratio (EVR) of the predator catch value supported by forage fish (x) to the total fishery catch value (excluding non-cephalopod invertebrates), which includes both predators and non-predators of forage fish (y) (Equation D-6).

$$EVR = \frac{x}{y} \quad \text{Eq. D-6}$$

Once an EVR for each of the 56 Ecopath models was calculated, we used it to estimate the total supportive value ($\$Supportive$) of forage fish at the larger scale for each EEZ and HSA. We multiplied the respective EVR by the total fishery catch value (excluding non-cephalopod invertebrates) provided by the Sea Around Us database ($\$SAUP$) for each EEZ and HSA (Equation D-7).

$$\$Supportive = EVR \times \$SAUP \quad \text{Eq. D-7}$$

In this extrapolation, we assumed that all Ecopath models were representative of the entire EEZ or HSA in which they resided or were adjacent to. In EEZs and HSAs where multiple Ecopath models existed, we calculated an EVR for each model and then calculated a weighted average for the entire EEZ or HSA, giving more weight to models with larger geographic coverage.

Once the supportive service values of forage fish were estimated for all EEZ and HSAs, we summed all of them up along with the direct forage fish catch values, producing a global estimate to marine fisheries value.

² In EEZ or HSA areas that did not have "Herring-likes" or "Anchovies" as functional groups, values by species groups were obtained if applicable.

APPENDIX E: Supplementary Figures and Tables

Figure E5.1
Forage Fish Catch Across all Ecopath Models by Volume.

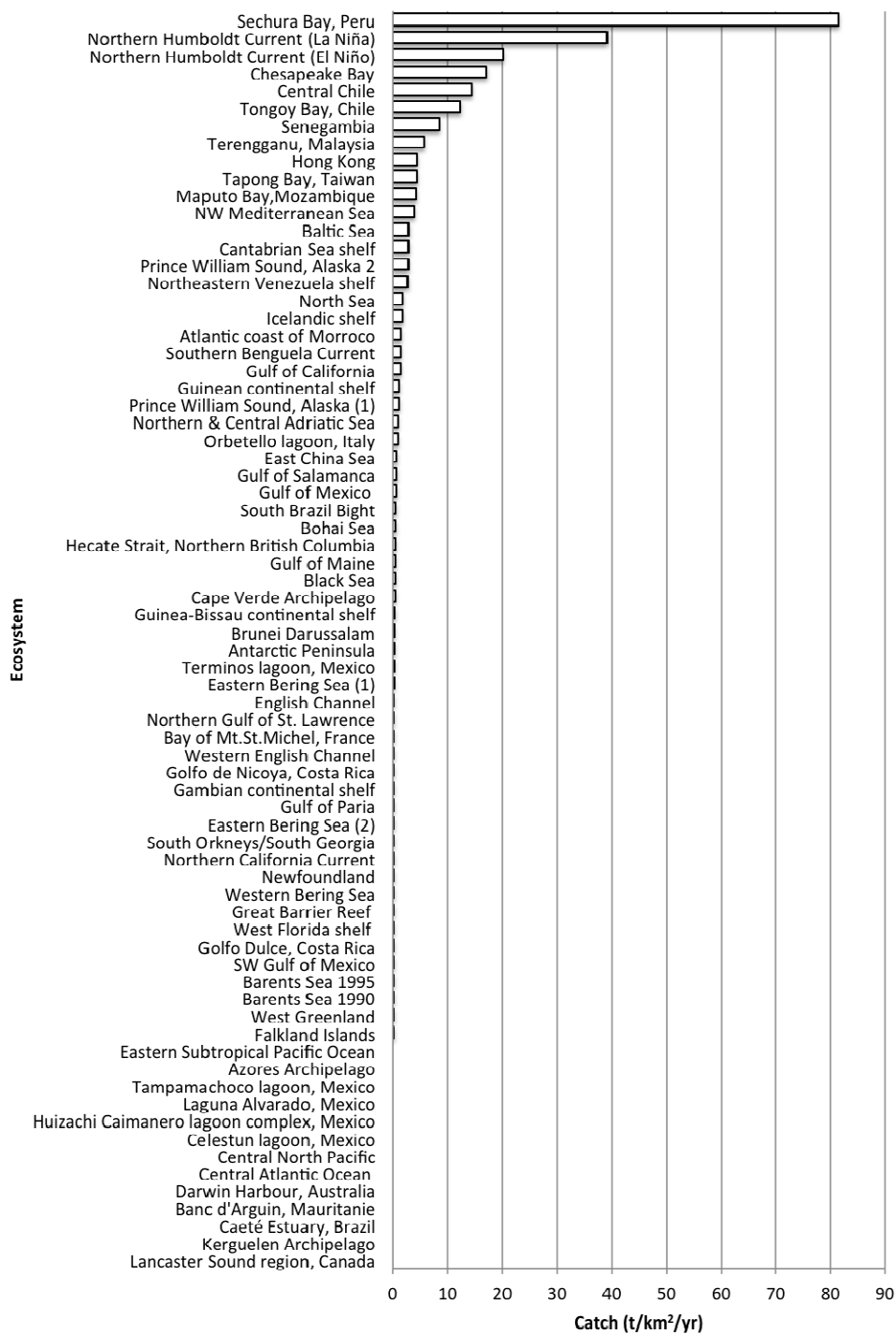


Figure E5.2

Supportive Contribution of Forage Fish to Other Fisheries Across all Ecopath Models by Volume.

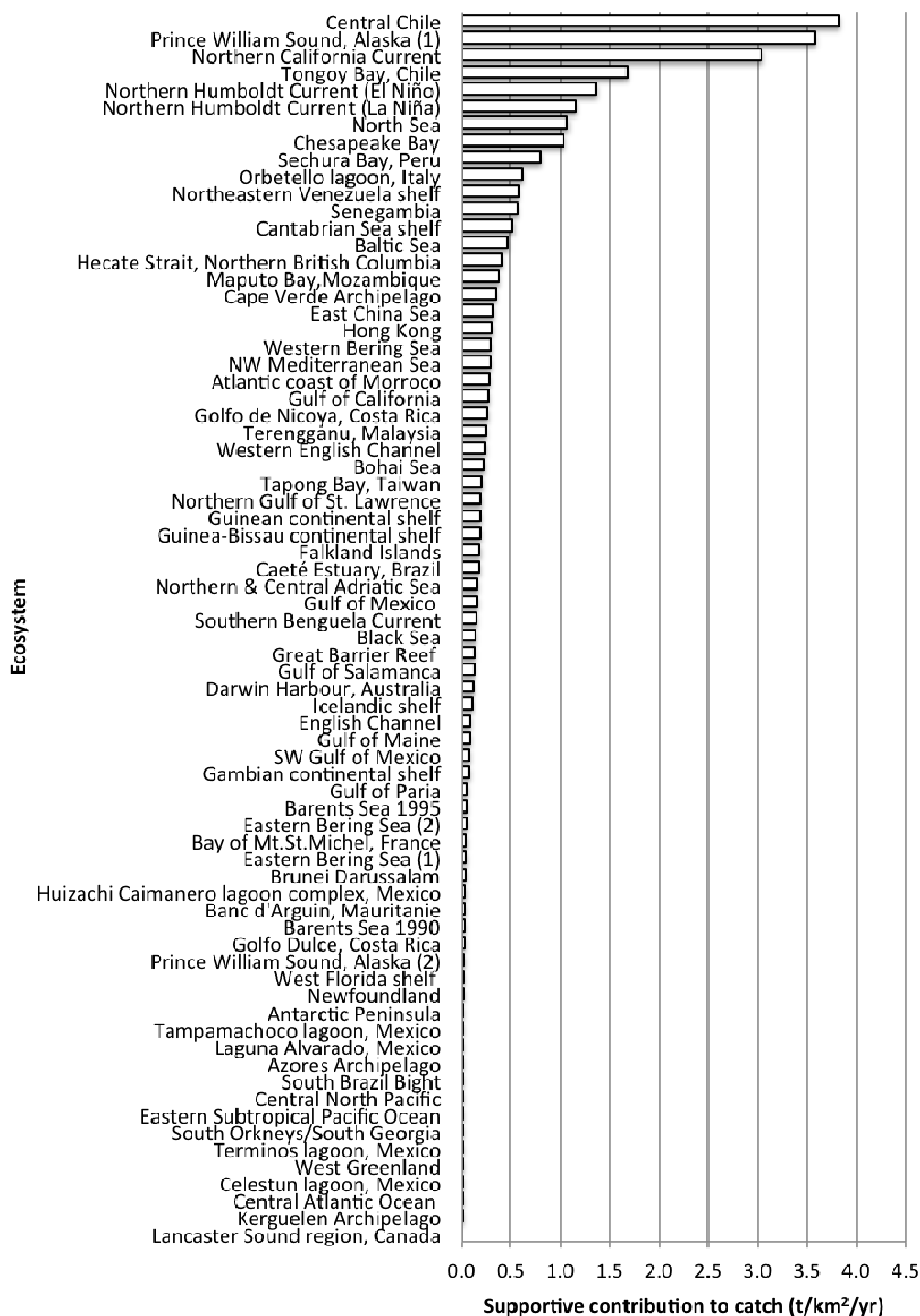


Figure E5.3

Mean Catch of Forage Fish (red) and Mean Contribution of Forage Fish to Other Species' Catch (gray) by Latitude with standard error plotted. (Upwelling groups were separated out to more clearly demonstrate latitudinal patterns.)

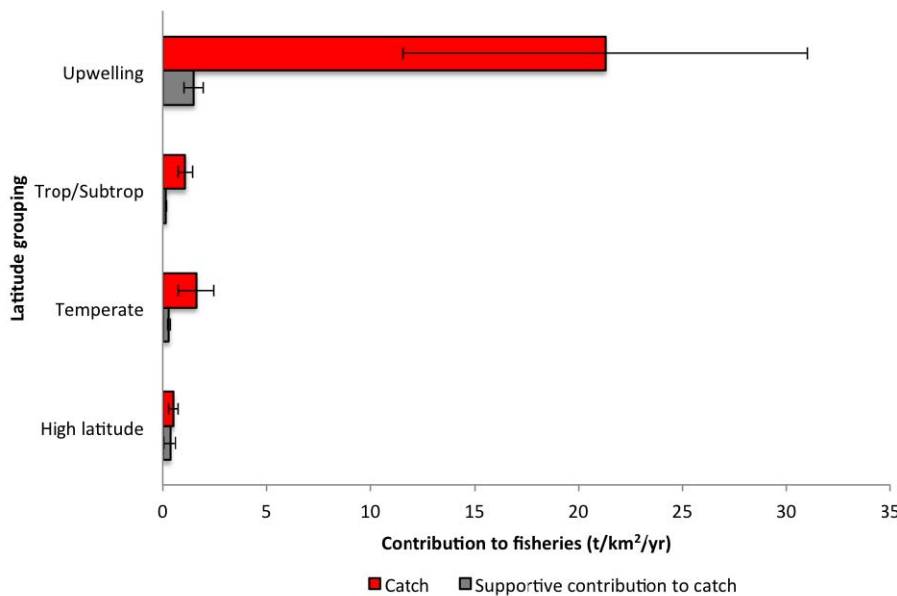


Figure E5.4

Cross-ecosystem Comparison of Mean Catch Value of Forage Fish (red) and Mean Contribution of Forage Fish to Other Species' Catch Value (gray) with standard error plotted.

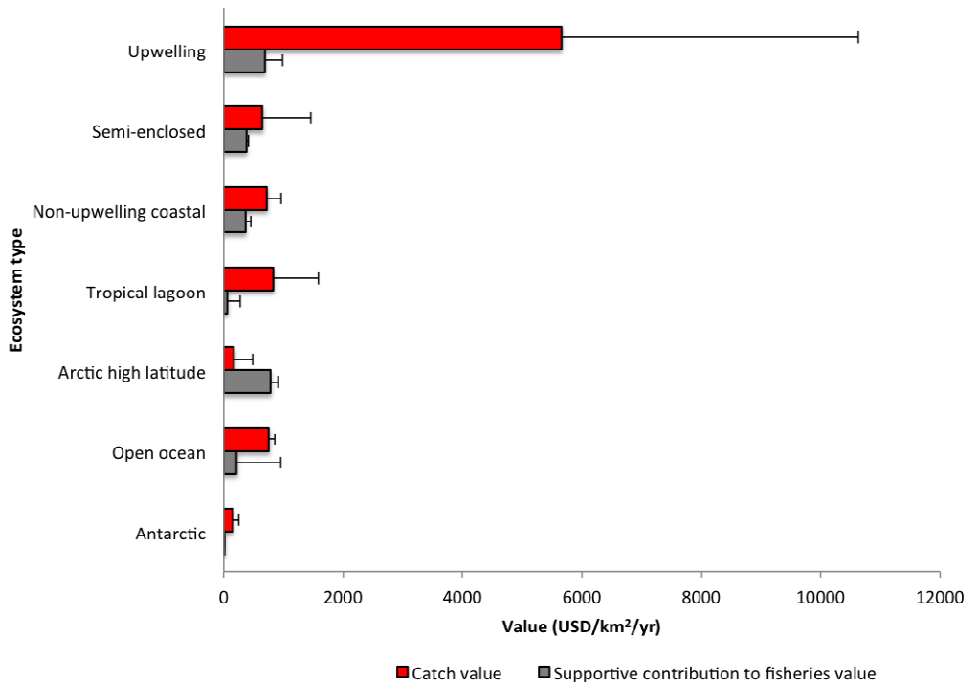


Figure E5.5

Supportive Contribution of Forage Fish to Ecosystem Predator Production Across all Ecopath Models.

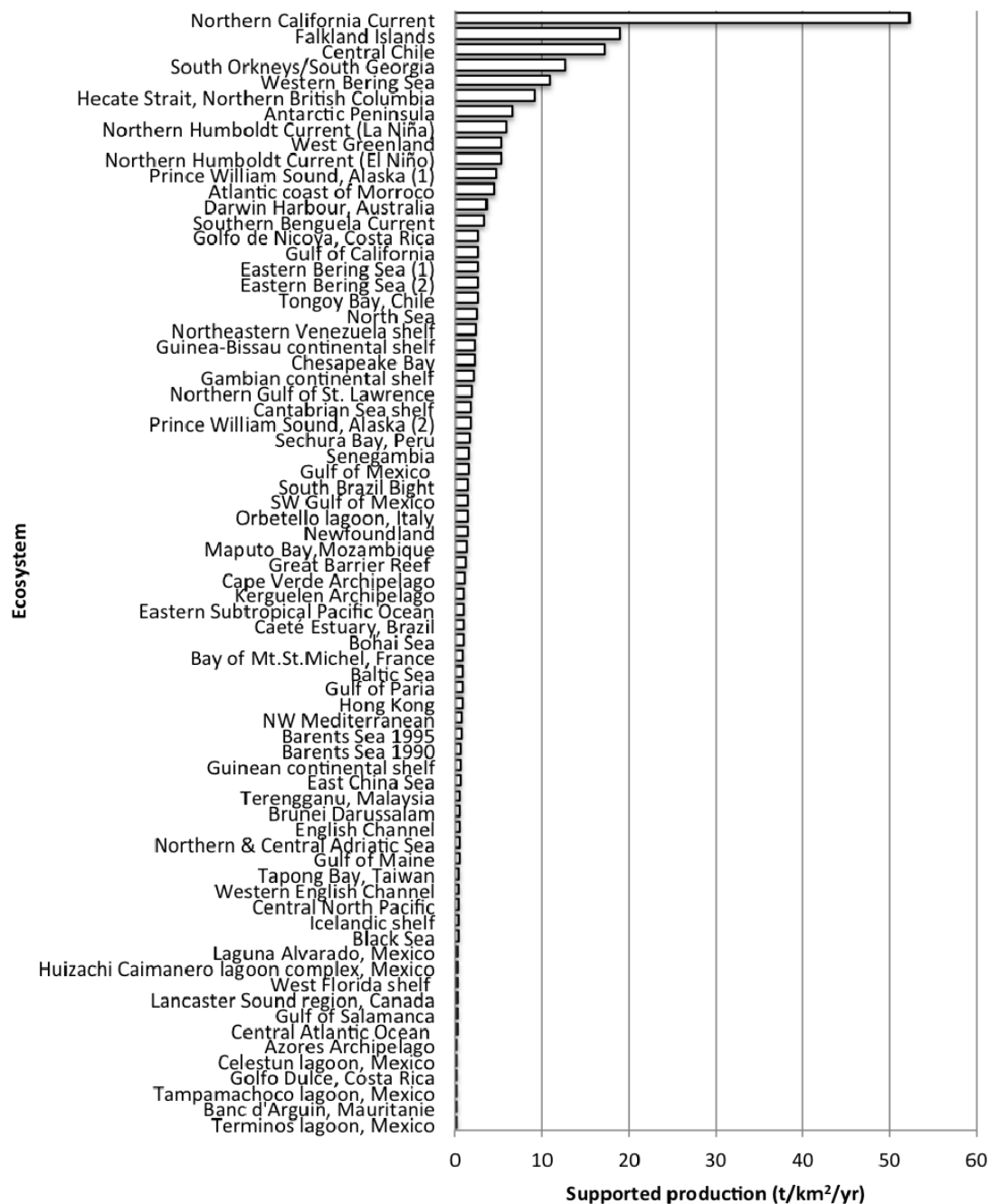


Figure E5.6

Mean Supportive Contribution of Forage Fish to (Non-commercial) Ecosystem Predator Production with standard error plotted.

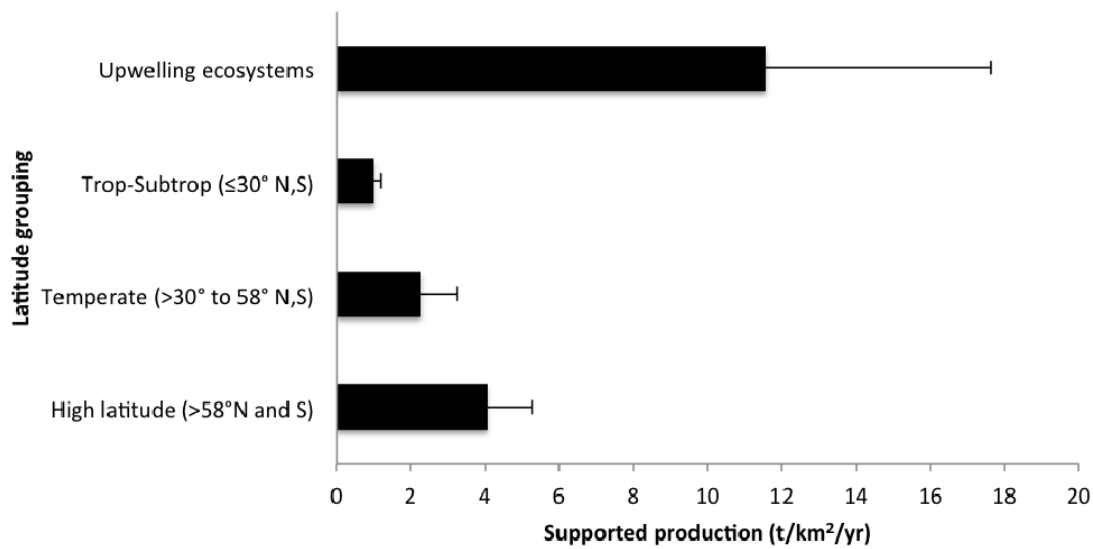


Figure E6.1
Locations of the Ecosystems Explored with EwE Model Simulations.

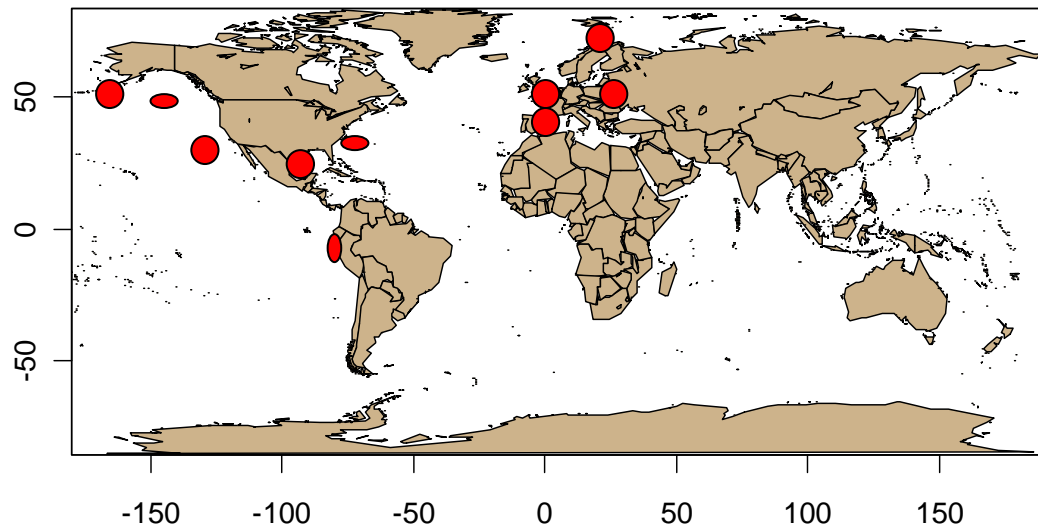


Table E-1

Ecopath Models used in Chapter 5 Analysis

#	Model Name	Model Year(s)	Latitude group	Ecosystem type	Value data	Citation
1	Western Bering Sea ^a	1980s-1990s	High latitude	Arctic high latitude	Y	Aydin et al. 2002
2	Eastern Bering Sea (1)	1980s	High latitude	Arctic high latitude	Y	Trites et al. 1999
3	Eastern Bering Sea (2)	1980s-1990s	High latitude	Arctic high latitude	Y	Aydin et al. 2002
4	Prince William Sound, Alaska (1) ^b	1980-1989	High latitude	Arctic high latitude	Y	Dalsgaard and Pauly 1997
5	Prince William Sound, Alaska (2) ^c	1994-1996	High latitude	Arctic high latitude	Y	Okey and Pauly (eds.) 1999
6	Hecate Strait, Northern British Columbia	2000	High latitude	Non-upwelling coastal	Y	Ainsworth 2002
7	Northern California Current	1990	Upwelling	Upwelling	Y	Field et al. 2006
8	Gulf of California	1978-1979	Tropical-Subtropical	Semi-enclosed	Y	Arrenguín-Sánchez et al. 2002
9	Huizachi Caimanero lagoon complex, Mexico	1970-2000	Tropical-Subtropical	Tropical lagoon	Y	Zetina-Rejón et al. 2003
10	Golfo de Nicoya, Costa Rica	1980s-1990s	Tropical-Subtropical	Tropical lagoon	Y	Wolff et al. 1998
11	Golfo Dulce, Costa Rica	1960-1990s	Tropical-Subtropical	Tropical lagoon	N	Wolff et al. 1996
12	Eastern Subtropical Pacific Ocean ^d	1993-1997	Tropical-Subtropical	Open ocean	Y	Olson and Watters 2003
13	Northern Humboldt Current ^e	1995-1996	Upwelling	Upwelling	Y	Tam et al. 2008
14	Northern Humboldt Current ^f	1997-1998	Upwelling	Upwelling	Y	Tam et al. 2008
15	Sechura Bay, Peru	1996	Upwelling	Upwelling	Y	Taylor et al. 2008
16	Central Chile	1998	Upwelling	Upwelling	Y	Neira et al. 2004
17	Tongoy Bay, Chile	1980s-1990s	Upwelling	Upwelling	N	Wolff 1994

18	Falkland Islands	1990s	Temperate	Non-upwelling coastal	Y	Cheung and Pitcher 2005
19	South Brazil Bight	1998-1999	Tropical-Subtropical	Non-upwelling coastal	Y	Gasalla and Rossi-Wongtschowski 2004
20	Caeté Estuary, Brazil	1999	Tropical-Subtropical	Non-upwelling coastal	Y	Wolff et al. 2000
21	Gulf of Paria	1980s-1990s	Tropical-Subtropical	Tropical lagoon	N	Manickchand-Heileman et al. 2004
22	Northeastern Venezuela shelf	1970s-1980s	Tropical-Subtropical	Non-upwelling coastal	Y	Mendoza 1993
23	Gulf of Salamanca	1997	Tropical-Subtropical	Tropical lagoon	Y	Duarte and García 2004
24	Celestun lagoon, Mexico	2001	Tropical-Subtropical	Tropical lagoon	Y	Vega-Cendejas and Arrenguín-Sánchez 2001
25	Terminos lagoon, Mexico	1980s-1990s	Tropical-Subtropical	Tropical lagoon	N	Manickchand-Heileman et al. 1998a
26	Southwestern Gulf of Mexico	1980s-1990s	Tropical-Subtropical	Tropical lagoon	N	Manickchand-Heileman et al. 1998b
27	Laguna Alvarado, Mexico	1991-1994	Tropical-Subtropical	Tropical lagoon	Y	Cruz-Escalona et al 2007
28	Tampamachoco lagoon, Mexico	1980s-1990s	Tropical-Subtropical	Tropical lagoon	N	Rosado-Solórzano and del Prío 1998
29	Gulf of Mexico	1950-2004	Tropical-Subtropical	Non-upwelling coastal	N	Walters et al. 2008
30	West Florida shelf	1980s-1990s	Tropical-Subtropical	Non-upwelling coastal	N	Okey et al. 2004
31	Chesapeake Bay	2000	Temperate	Non-upwelling coastal	Y	Christensen et al. 2009
32	Gulf of Maine	1977-1986	Temperate	Non-upwelling coastal	Y	Heymans 2001
33	Northern Gulf of St. Lawrence	1985-1987	Temperate	Non-upwelling coastal	Y	Morissette et al. 2003
34	Newfoundland	1995	Temperate	Non-upwelling coastal	Y	Heymans and Pitcher 2002
35	Lancaster Sound region, Canada	1980s	High latitude	Arctic high latitude	N	Mohammed 2001
36	West Greenland	1991-	High latitude	Arctic high	Y	Pedersen 1992

		1992		latitude		
37	Icelandic shelf	1997	High latitude	Arctic high latitude	N	Mendy 1999
38	Barents Sea (1)	1990	High latitude	Arctic high latitude	Y	Blanchard et al. 2002
39	Barents Sea (2)	1995	High latitude	Arctic high latitude	Y	Blanchard et al. 2002
40	Baltic Sea	1974-2000	Temperate	Semi-enclosed	Y	Harvey et al. 2003
41	North Sea	1981	Temperate	Non-upwelling coastal	Y	Christensen 1995
42	English Channel	1995	Temperate	Non-upwelling coastal	Y	Stanford and Pitcher 2004
43	Western English Channel	1994	Temperate	Non-upwelling coastal	Y	Araújo et al. 2005
44	Bay of Mt.St.Michel, France	2003	Temperate	Non-upwelling coastal	Y	Arbach Leloup et al. 2008
45	Cantabrian Sea shelf	1994	Temperate	Non-upwelling coastal	Y	Sánchez and Olaso 2004
46	Azores Archipelago	1997	Temperate	Non-upwelling coastal	Y	Guénette and Morato 2001
47	Northwestern Mediterranean Sea	1994	Temperate	Semi-enclosed	Y	Coll et al. 2006
48	Orbetello lagoon, Italy	1996	Temperate	Non-upwelling coastal	Y	Brando et al. 2004
49	Northern & Central Adriatic Sea	1990s	Temperate	Semi-enclosed	Y	Coll et al. 2007
50	Black Sea	1989-1991	Temperate	Semi-enclosed	Y	Örek 2000
51	Atlantic coast of Morocco	1984	Upwelling	Upwelling	Y	Stanford et al. 2004
52	Banc d'Arguin, Mauritanie	1988-1998	Tropical-Subtropical	Non-upwelling coastal	Y	Sidi and Diop 2004
53	Cape Verde Archipelago	1981-1985	Tropical-Subtropical	Non-upwelling coastal	Y	Stobberup et al. 2004
54	Central Atlantic Ocean	1997-1998	Temperate	Open ocean	Y	Vasconcellos and Watson 2004

55	Gambian continental shelf	1995	Tropical-Subtropical	Non-upwelling coastal	N	Mendy 2004
56	Guinea-Bissau continental shelf	1990-1992	Tropical-Subtropical	Non-upwelling coastal	Y	Amorim et al. 2004
57	Senegambia	1990	Tropical-Subtropical	Non-upwelling coastal	Y	Samb and Mendy 2004
58	Guinean continental shelf	2005	Tropical-Subtropical	Non-upwelling coastal	Y	Gascuel et al. 2009
59	Southern Benguela Current	1990	Upwelling	Upwelling	Y	Shannon et al. 2003
60	South Orkneys/South Georgia	1990s	High latitude	Antarctic	Y	Bredesen 2004
61	Antarctic Peninsula	1991-2001	High latitude	Antarctic	Y	Erfan and Pitcher 2005
62	Kerguelen Archipelago EEZ	1987-1988	Temperate	Non-upwelling coastal	Y	Pruvost et al. 2005
63	Maputo Bay, Mozambique	1980s-1990s	Tropical-Subtropical	Non-upwelling coastal	Y	Paula e Silva et al. 1993
64	Great Barrier Reef, Australia	2000	Tropical-Subtropical	Tropical lagoon	N	Gribble 2005
65	Darwin Harbour, Australia	1990-2000	Tropical-Subtropical	Non-upwelling coastal	N	Martin 2005
66	Brunei Darussalam	1989-1990	Tropical-Subtropical	Tropical lagoon	Y	Silvestre et al. 1993
67	Terengganu, Malaysia	1980s	Tropical-Subtropical	Tropical lagoon	Y	Liew and Chan 1987
68	Hong Kong, China	1990s	Tropical-Subtropical	Non-upwelling coastal	N	Buchary et al. 2002
69	Tapong Bay, Taiwan	1999-2001	Tropical-Subtropical	Tropical lagoon	N	Lin et al. 2006
70	East China Sea	1997-2000	Tropical-Subtropical	Open ocean	Y	Jiang et al. 2008
71	Bohai Sea	1982-1983	Temperate	Non-upwelling coastal	Y	Tong et al. 2000
72	Central North Pacific	1990s	Tropical-Subtropical	Open ocean	N	Cox et al. 2002
^a 48 group model		^d ETP7 model				

^b pre-oil spill model	^e La Niña model	
^c post-oil spill model	^f El Niño model	

Table E-2
Forage Fish Species Contained in Ecopath Model Groups used in Chapter 5.

#	Common Name:	Scientific Name:
1	Whitebait smelt	<i>Allosmerus elongatus</i>
2	Blueback	<i>Alosa aestivalis</i>
3	Azov shad	<i>Alosa caspia</i>
4	Twaite shad	<i>Alosa fallax</i>
5	Hickory shad	<i>Alosa mediocris</i>
6	Pontic shad	<i>Alosa pontica</i>
7	Alewife	<i>Alosa pseudoharengus</i>
8	American shad	<i>Alosa sapidissima</i>
9	American sand lance	<i>Ammodytes americanus</i>
10	Northern sand lance	<i>Ammodytes dubius</i>
11	Pacific sand lance	<i>Ammodytes hexapterus</i>
12	Lesser sandeel	<i>Ammodytes marinus</i>
13	Sandeel	<i>Ammodytes spp.</i>
14	Small sandeel	<i>Ammodytes tobianus</i>
15	Broad-striped anchovy	<i>Anchoa hepsetus</i>
16	Bright Anchovy	<i>Anchoa lucida</i>
17	Bay anchovy	<i>Anchoa mitchilli</i>
18	Longnose anchovy	<i>Anchoa nasus</i>

19	Spicule Anchovy	<i>Anchoa spinifer</i>
20	Anchovies	<i>Anchoa</i> spp.
21	Greater argentine	<i>Argentina silus</i>
22	Argentines	<i>Argentine</i> spp.
23	Big-scale sand smelt	<i>Atherina boyeri</i>
24	Sand smelt	<i>Atherina presbyter</i>
25	Silversides	Atherinidae
26	Gulf menhaden	<i>Brevoortia patronus</i>
27	Atlantic menhaden	<i>Brevoortia tyrannus</i>
28	Jacks and pompanos	Carangidae (<i>excluding Decapterus, Selar, Alepes, Selaroides, Megalaspis</i>)
29	Grooved razor-fish	<i>Centriscus scutatus</i>
30	Atlantic anchoveta	<i>Cetengraulis edentulus</i>
31	Atlantic Herring	<i>Clupea harengus harengus</i>
32	Pacific herring	<i>Clupea pallasii pallasii</i>
33	Clupeids	Clupeidae
34	Osbeck's grenadier anchovy	<i>Coilia mystus</i>
35	Anchovies	Engraulidae
36	Cape Anchovy	<i>Engraulis capensis</i>
37	European anchovy	<i>Engraulis encrasicolus</i>
38	Japanese anchovy	<i>Engraulis japonicas</i>
39	Northern Anchovy	<i>Engraulis mordax</i>
40	Peruvian anchoveta	<i>Engraulis ringens</i>
41	Bonga shad	<i>Ethmalosa fimbriata</i>
42	Red-eye round herring	<i>Etrumeus teres</i>

43	Whitehead's round herring	<i>Etrumeus whiteheadi</i>
44	Krill	<i>Euphausia superb</i>
45	Euphausiids	<i>Euphausia vallentini</i>
46	Krill	Euphausiacea
47	Flyingfishes	Exocoetidae
48	Scaled Sardine	<i>Harengula jaguana</i>
49	Halfbeaks	Hemiramphidae
50	Five spot herring	<i>Hilsa kelee</i>
51	Halfbeaks	<i>Hyphorhamphus</i> spp.
52	African ilisha	<i>Ilisha africana</i>
53	Dotted Gizzard Shad	<i>Konosirus punctatus</i>
54	Sabretooth anchovy	<i>Lycengraulis</i> sp.
55	Capelin	<i>Mallotus villosus</i>
56	Silversides	<i>Membras</i> spp.
57	Golden silverside	<i>Menidia colei</i>
58	Atlantic silverside	<i>Menidia menidia</i>
59	Silversides	<i>Menidia</i> spp.
60	Neotropical silverside	<i>Neopisthopterus tropicus</i>
61	Neotropical silverside	<i>Odontesthes nigricans</i>
62	Chilean silverside	<i>Odontesthes regia regia</i>
63	Threadfin Herring	<i>Opisthonema oglinum</i>
64	Herrings	<i>Opisthophterus</i> spp.
65	Smelts	Osmeridae
66	Rainbow smelt	<i>Osmerus mordax</i>
67	Atlantic rainbow smelt	<i>Osmerus mordax mordax</i>

68	Bigwing halfbeak	<i>Oxyporhamphus micropterus</i>
69	Indian pellona	<i>Pellona ditchela</i>
70	American coastal pellona	<i>Pellona harroweri</i>
71	Atlantic butterfish	<i>Peprilus triacanthus</i>
72	Blueback herring	<i>Pomolobus aestivalis</i>
73	Alewife	<i>Pomolobus pseudoharengus</i>
74	Sardina	<i>Sardina</i>
75	European pilchard	<i>Sardina pilchardus</i>
76	Round sardinella	<i>Sardinella aurita</i>
77	Brazilian sardinella	<i>Sardinella brasiliensis</i>
78	Madeiran sardinella	<i>Sardinella maderensis</i>
79	Sardinellas	<i>Sardinella</i> spp.
80	Japanese sardinella	<i>Sardinella zunasi</i>
81	Cape sardine	<i>Sardinops sagax</i>
82	South American pilchard	<i>Sardinops sagax sagax</i>
83	Hair-fin anchovy	<i>Setipinna tary</i>
84	Falkland sprat	<i>Sprattus fuegensis</i>
85	Sprat	<i>Sprattus sprattus</i>
86	Indian anchovy	<i>Stolephorus</i> spp.
87	Araucanian herring	<i>Strangomeria bentincki</i>
88	Eulachon	<i>Thaleichthys pacificus</i>
89	Kammal thyssa	<i>Thryssa kammalensis</i>
90	Euphausiids	<i>Thysanoessa inermis</i>
91	Euphausiids	<i>Thysanoessa raschi</i>
92	Euphausiids	<i>Thysanoessa</i> spp.

APPENDIX F: Descriptions of EwE Models Used in Chapter 6

For each Ecopath with Ecosim (EwE) model, we identified the forage fish species among the models’ “functional” groups. Forage fish species in EwE models are grouped separately as a single species, in a group of species, or both. The grouping of species was assigned by the model authors and for the purposes of this meta-analysis, they were not changed. Only groups comprised solely of forage fish were considered in our analysis. For instance, if an anchovy species was a component of a model group called “Small Pelagics” along with gobies and juvenile mackerels, this group was not considered a forage fish group because gobies and juvenile mackerels did not meet our definition of forage fish.

(1) Aleutian Islands and (2) Southeast Alaska

Ecosystem—The Aleutian Islands and Southeast Alaska marine ecosystems collectively experience subarctic conditions with strong seasonal and multi-decadal climate oscillations (Peterson and Schwing 2003). These cold and nutrient rich waters support a wide diversity of organisms, many of which are commercially important to fisheries (Boeing and Duffy-Angerson 2008, NMFS 2009). The forage species sustain marine mammal and seabird predators and are the target for some of the largest fisheries in this region. The Pacific herring fishery is the largest pelagic fishery in Alaska, having expanded as a direct result of increasing demand for fishmeal and fish oil for feeds (NMFS 2009).

EwE model—Guénette *et al.* (2006) developed two EwE models, one for the Aleutian Islands and one for Southeast Alaska, to test hypotheses for the decline of Steller sea lions since the late 1970s. Both models were specifically oriented at understanding the dynamics between sea lions and transient killer whales in Southeast Alaska and the Aleutian Islands. The main objectives of these models were to reproduce the observed time series of species abundance and to examine the possibility that transient killer whales were responsible for the decline of Steller sea lions. The model for the Aleutian Islands included 40 functional groups of which we modeled 3 functional groups of forage fish species common to the region. Similarly, the Southeast Alaska model included 40 functional groups of which we modeled 3 forage fish species.

(3) Baltic Sea

Ecosystem—The Baltic Sea, a brackish, highly productive, semi-enclosed sea with a temperate climate, is specifically characterized by extremely low species diversity (Johannesson *et al.* 2011). The major stressors to ecosystem function include intensive fishing, eutrophication, and climate change (Neumann 2010, UNEP 2005). The dominant commercial fisheries are cod, herring, and sprat.

EwE model—The Baltic Sea model used in this meta-analysis was developed by Hansson *et al.* (2007) based on an earlier EwE model by Harvey *et al.* (2003). This updated model was created to explore possible food web responses caused by fisheries and nutrient changes in the Baltic Sea. The model used historical data (1974-2000) and calibrated the model to fit historical fishing patterns and estimated recruitment. Sixteen functional groups were included in the EwE model, of which juvenile and adult herring and sprat were the forage fish species for the region.

(4) Barents Sea

Ecosystem—The Barents Sea is a moderately productive, ice-edge ecosystem strongly influenced by variable Atlantic Ocean inflow, alternating climate regimes, and ongoing climate change (Gaichas *et al.* 2009, Hunt and Megrey 2005, www.indiseas.org). Atlantic cod, capelin, and herring are a key triad of species that are linked by predator-prey relationships (Gjøsæter *et al.* 2009, Olsen *et al.* 2010). Capelin is the most abundant forage fish in the Barents Sea (ICES 2010).

EwE model—The Barents Sea model was developed to investigate the interactions between cetacean predators, their prey, and fisheries (Blanchard *et al.* 2002). Blanchard *et al.* created two separate ecosystem models to depict scenarios of both high and low capelin abundance in the Barents Sea. Our EwE model simulations were run using the parameters for the low capelin abundance scenario. This model included 41 functional groups, of which 5 functional groups were made up of forage fish. Juvenile and adult herring and capelin represented 4 of the 5 forage fish model groups, and the remaining forage fish group was an aggregated group of species named “pelagic planktivores.”

(5) Chesapeake Bay

Ecosystem—The Chesapeake Bay is an extremely productive, partially mixed estuary that supports a myriad of coastal species. Severe nutrient loading, hypoxia, and the loss of ecologically important habitat are among the major issues affecting the bay and

its biological resources (Ruhl and Rybicki 2010). Furthermore, many fish and shellfish populations face the additional stress of heavy exploitation by fisheries.

EwE model—The Chesapeake Bay Fisheries Ecosystem Model was created in response to a need for improved estimation of trophic pathways in the Chesapeake region to aid management (Christensen *et al.* 2009). This model attempted to understand the impacts of fisheries on both target and non-target species and was been proposed as a viable tool to answer a variety of questions for coastal managers in the Chesapeake Bay (Christensen *et al.* 2008). In total there were 45 functional groups, consisting of separate species, various life stages of species, and aggregated groups of species of which we modeled 3 forage fish groups.

(6) Gulf of Mexico

Ecosystem—The Gulf of Mexico is a large, moderately productive, semi-enclosed coastal water body, which supports lucrative multispecies fisheries. Habitat degradation, eutrophication, hypoxia, hydrocarbon pollution, and fisheries overexploitation are some of the major stressors to the Gulf of Mexico (Turner *et al.* 2008). Commercial and recreational fisheries are considered to be the primary cause of biomass changes for marine species, and climate variability is a secondary cause (Sherman 2003). Many fisheries are considered overexploited, and substantial declines (near 90%) have been found for some large pelagic fish (Baum and Myers 2004). Gulf menhaden represent the largest forage fish fishery in the Gulf of Mexico, and are the second largest fishery (by weight) in the United States (Vaughan *et al.* 2007).

EwE model—The Gulf of Mexico model was originally developed as an EwE model for Tampa Bay, Florida. Walters *et al.* (2006) developed this model further to include other coastal areas of the Gulf of Mexico. The model had 62 functional groups. Ten key species were represented by detailed, multi-stanza population dynamics models to explicitly account for any possible changes in recruitment due to changes in bycatch and trophic interactions. This model did not include seabirds or marine mammals, and was limited to the coastal areas of the northern Gulf of Mexico. There were four forage fish species groups in this model.

(7) Northern California Current

Ecosystem—The Northern California Current occupies the northernmost extent of the California coastal upwelling current. Primary productivity is mainly driven by the upwelling of cold nutrient rich waters, which varies in magnitude, duration, and geographic location as a result of the seasonal, annual, and multi-decadal climate variability (Largier *et al.* 2006). Likewise, species at each successively higher trophic level may fluctuate as a result of bottom-up forces, particularly forage fish (Bakun 1993, Dorman *et al.* 2011, NMFS 2009). The California current has a long history of forage fish fisheries, which include Pacific sardine, Northern anchovy, Pacific herring, and Pacific hake (NMFS 2009).

EwE model—Field *et al.* (2006) developed an EwE model of the Northern California Current to investigate the relationships among physical, ecological and human (i.e., fisheries) processes influencing commercial stocks of fish and shellfish. In particular the authors wanted to evaluate relationships between climate variability and certain species of rockfish, shrimp, and crab. There were two models created, one based on parameters from the 1960s and another based on the 1990s. We used the model with the latter parameters, which included a total of 65 functional groups and 3 forage fish groups.

(8) Northern Humboldt Current

Ecosystem—The nutrient rich upwelling waters of the Humboldt Current support the world's largest fishery, the Peruvian anchoveta (FAO 2010). Similar to other eastern boundary current upwelling ecosystems, productivity is tightly linked to variability in climate from seasonal to multi-decadal time scales, including El Niño–Southern Oscillation (Alheit and Niquen 2004, Chavez *et al.* 2008). While forage fish species represent the majority of historical and current catch values in terms of tonnage, they also continue to serve as essential prey for many higher trophic predators (Chavez *et al.* 2008).

EwE model—The Northern Humboldt Current EwE model was created to assess the contributions of external drivers (i.e., phytoplankton fluctuations, fish immigration, and fishing intensity) versus internal control mechanisms (i.e., predator-prey dynamics) during an El Niño–Southern Oscillation cycle (Taylor *et al.* 2008). It was based on a model originally produced by Tam *et al.* (2008), and specifically focused on elucidating the most important drivers of the Peruvian anchoveta fishery using time series data from 1995 to 2004. There were 33 functional groups represented, and we analyzed 2 forage fish species groups from it.

(9) North Sea

Ecosystem—The North Sea is a continental shelf sea with a diversity of tidal, upwelling, and riverine fronts , which support its relatively high primary productivity (Belkin *et al.* 2009; McGinley 2008). Fishing is the primary driving force for biomass change in this ecosystem, followed by variations in climate (Sherman 2003). Forage fish, particularly the sand eel, support a wide variety of predators and are targeted by reduction fisheries (Wanless *et al.* 2007).

EwE model—Mackinson and Daskalov (2007) created the ecosystem model of the North Sea to support an ecosystem approach to fisheries management. The specific objectives of this model were to improve on previous models in terms of resolution, trophic connections, spatial structure of species, and to make comparisons with historical dynamics. This model had 68 functional groups, including 3 forage fish species.

(10) Western English Channel

Ecosystem—The English Channel is a shallow stretch of continental shelf between contiguous Europe and England, and is characterized by strong tides and temperate climate. In the Western English Channel, annual sea surface temperatures have undergone considerable change in the last century leading to changes and fluctuations in plankton and fish communities (Hawkins *et al.* 2003). Fisheries in the English Channel represent many nations, multiple gear types, and target multiple species (Ulrich *et al.* 2002). Commercial and recreational fishermen catch many species in the English Channel, however only a handful of these are managed by catch limits.

EwE model—Araujo *et al.* (2005) created two Western English Channel models based on a previous model by Stanford and Pitcher (2004). The Western English Channel models were created for warm and cold sea surface temperature regimes. They were used to explore the effects that fishing, trophic interactions, and variability in plankton production have on the observed variation in fish abundance. We used the 1994 model with the warmer sea surface in our analysis. This model had 52 functional groups of which 4 were forage fish groups.

APPENDIX G: EwE Management Strategy Evaluation (MSE) module

The module is an external spreadsheet that allows for multiple runs of an EwE model to occur at once, with all output compiled into external comma-separated values (CSV) files. The runs may represent different fishing mortalities, different yields, and/or different upper and lower thresholds for the step and hockey stick management strategies. The runs may also be different simulations, given a pre-specified error variance, of the same strategy. This variance is given as a coefficient of variation ($CV = \frac{SE(\theta)}{\theta}$), and provides both observation error and process error as the same value. The intended values for the fishing mortality rates varied from species to species due to species-specific differences in life history parameters.

The module treated the user-defined fixed fishing mortalities as targets to set annual quotas. The target fishing mortality was achieved by estimating the effort for a desired fishing mortality or yield in a constant yield framework. For each year of the EwE model, the fishing quota was updated using predicted biomass from a stock assessment model. The stock assessment models added recruitment based on the biomass of the previous year and the stock recruitment curves. The CV term for the observation and process error was included in this annual stock assessment. For each time step of EwE, the module set the target fishing mortality for the year by capping the fishing effort using the biomass from the current time step.

Through the module, one may also change the standard deviation for the primary production variance; the control type (weak, strong or selective stocks) of the target species' fishing fleets; and the type of primary production forcing function. These uses were not applied or changed in the work in this chapter.

The possible output files include biomasses, yields, consumption levels, feeding times, the realized fishing mortalities, and the realized predation rates. This output is produced for each species and species group of the inputted ecosystem for every month of each simulation run. We looked at the yearly averages that resulted from the monthly numbers.

APPENDIX H: A Synthesis of the Joint Effects of Depletion of Forage Fish Biomass and Predator Diet Dependency (The PREP Equation)

In order to determine the parameters of Eq. (1), the PREP equation, we recast it as a linear statistical model:

$$\ln[R] = \ln[\rho] + \alpha \ln[D] + \beta \ln\left[1 - \frac{B}{B_0}\right] + \varepsilon \quad (\text{Eq. H-1})$$

If we assumed that the parameters governing the response were identical across systems and the responses of all species in all systems at different fishing levels were independent, we could estimate the parameters by standard linear regression. Three aspects of the data influenced its error. First, different ecosystems may require different parameters. Second, EwE models are based on the idea of biomass conservation; when one species increases, some others must decrease to keep the total biomass roughly the same. Therefore, the responses of species in the system cannot be independent, but must instead be negatively correlated. Third, the data consist of model results for the same species at different fishing levels. All else being equal, the response of a given species at two very similar fishing levels must be more similar than the responses at two widely different fishing levels. Therefore the responses of a single species at different fishing levels cannot be independent, but should instead be positively correlated.

To account for these features of the data, we developed a hierarchical regression model with non-independent errors. The rationale of the approach is to assert that the parameters for different systems come from common distributions and that the errors (ε in Eq. H-1) are positively correlated across fishing levels and negatively correlated across species within a system at a given fishing level.

Description of model error structure

For a particular species j in system s at depletion level B , the response $R_{j,s,B}$ is:

$$\ln[R_{j,s,B}] = \ln[\rho_s] + \alpha_s \ln[D_{j,s}] + \beta_s \ln\left[1 - \frac{B}{B_0}\right] + \varepsilon_{j,s,B} \quad (\text{Eq. H-2})$$

We made the model hierarchical by making the coefficients system specific, while asserting that they come from a common distribution. That is, the system-specific parameter vectors, $\boldsymbol{\theta}_s = \{\ln(\rho_s), \alpha_s, \beta_s\}$, are independent, and normally distributed with mean vector $\boldsymbol{\mu}$ and covariance matrix Σ :

$$\begin{aligned} \boldsymbol{\theta}_s &\sim N(\boldsymbol{\mu}, \Sigma) \\ \boldsymbol{\mu} &= \{\mu_\rho, \mu_\alpha, \mu_\beta\} \\ \Sigma &= \begin{bmatrix} \sigma_\rho^2 & 0 & 0 \\ 0 & \sigma_\alpha^2 & 0 \\ 0 & 0 & \sigma_\beta^2 \end{bmatrix} \end{aligned} \quad (\text{Eq. H-3})$$

To model the correlation across depletion levels, we assumed a smooth function of depletion level that can be approximated by a differentiable Gaussian process. A common correlation function that guarantees differentiable responses is the squared exponential, $e^{-\varphi|B-B'|^2}$, where parameter φ governs the scale over which responses between depletion levels become independent, and B and B' are two depletion levels. For small φ , responses are similar over a wide range of depletion levels, while for large φ , the responses are effectively independent.

To account for the negative correlation among species within a system, we asserted that the sum of the ε 's across species within a system at a fixed depletion level was approximately constant. Within a system with n species, fixing the sum of the ε 's resulted in a constant correlation across species of $-1/(n-1)$. Unfortunately this rendered the n -species covariance matrix

singular because it occupied a space of $n-1$ dimensions. To avoid this we assumed that the sum of ε 's for the n species in the system was not quite constant, but was instead normally distributed with some small variance. This was analogous to imagining that the sum of ε 's across $n+v$ species would be exactly constant where the parameter v corresponds to ‘excess degrees of freedom’ and represents how strongly biomass conservation must be obeyed in the system. This led to a constant negative correlation across species of $-1/(n + v - 1)$. The correlation between species i and j is:

$$\text{corr}(\varepsilon_i, \varepsilon_j) = 1 - (1 - \delta_{ij}) \frac{n+v}{n+v-1} \quad (\text{Eq. H-4})$$

where δ_{ij} is the Kronecker delta which takes value 1 if $i=j$ and 0 otherwise. As $v \rightarrow 0$, biomass conservation is exact and as $v \rightarrow \infty$, biomass conservation is eliminated, allowing species to be effectively independent.

Putting these two sources of correlations together, we arrived at the covariance function

$$\text{cov}(\varepsilon_{i,s,B}, \varepsilon_{j,s',B'}) = \sigma_\varepsilon^2 e^{-\varphi|B-B'|^2} \left(1 - (1 - \delta_{ij}) \frac{n_s+v}{n_s+v-1}\right) \delta_{s,s'} \quad (\text{Eq. H-5})$$

where $\varepsilon_{i,s,B}$ is the residual for species i in system s at depletion level B and n_s is the number of species in system s . The $\delta_{s,s'}$ term is again the Kronecker delta and indicates that the responses of different systems are independent.

Methods of parameter estimation

We estimated parameters by maximum likelihood, carried out in two stages. The first stage maximized the likelihood for the system-specific regression parameters, $\{\mu_\rho, \mu_\alpha, \mu_\beta\}$, conditional on the variance and covariance terms. In the second stage, the variance and covariance parameters, $\{\sigma_\varepsilon^2, \varphi, v, \sigma_\rho^2, \sigma_\alpha^2, \sigma_\beta^2\}$, were estimated by numerically maximizing the likelihood given the maximum likelihood estimates for the regression parameters. Algorithmic details are provided below.

The log-likelihood for this model is given by

$$\ln[L] = -\frac{S}{2} \ln[\Sigma] - \frac{1}{2} \sum_{s=1}^S \ln [\mathbf{C}_s] - \frac{1}{2} \sum_{s=1}^S (\mathbf{y}_s - \mathbf{X}_s \boldsymbol{\theta}_s)' \mathbf{C}_s^{-1} (\mathbf{y}_s - \mathbf{X}_s \boldsymbol{\theta}_s) - \frac{1}{2} \sum_{s=1}^S (\boldsymbol{\theta}_s - \boldsymbol{\mu})' \Sigma^{-1} (\boldsymbol{\theta}_s - \boldsymbol{\mu}) \quad (\text{Eq. H-6})$$

where S is the total number of ecosystems, Σ is the covariance matrix from Eq. (H-3), \mathbf{C}_s is the system-specific covariance matrix as defined by Eq. (H-5), vector \mathbf{y}_s represents all of the responses for system s , matrix \mathbf{X}_s represents the collection of independent variables, i.e. $\mathbf{X}_{s\{j,B\}} = \{1, \ln[D_{j,s}], \ln[1 - \frac{B}{B_0}]\}$, $\boldsymbol{\theta}_s$ are the system-specific parameter estimates, and $\boldsymbol{\mu}$ is the vector of mean parameter estimates.

After some calculus and algebra, the maximum likelihood estimates for $\boldsymbol{\mu}$ and $\boldsymbol{\theta}_s$ conditional on the variance and covariance parameters are given by:

$$\boldsymbol{\mu} = \left[S\mathbf{I} - \sum_{s=1}^S (\mathbf{I} + \Sigma \mathbf{X}_s' \mathbf{C}_s^{-1} \mathbf{X}_s)^{-1} \right]^{-1} \sum_{s=1}^S [\mathbf{I} - (\mathbf{I} + \Sigma \mathbf{X}_s' \mathbf{C}_s^{-1} \mathbf{X}_s)^{-1}] \boldsymbol{\psi}_s \quad (\text{Eq. H-7})$$

and

$$\boldsymbol{\theta}_s = \boldsymbol{\psi}_s + (\mathbf{I} + \Sigma \mathbf{X}_s' \mathbf{C}_s^{-1} \mathbf{X}_s)^{-1} (\boldsymbol{\mu} - \boldsymbol{\psi}_s) \quad (\text{Eq. H-8})$$

where $\boldsymbol{\psi}_s = (\mathbf{X}_s' \mathbf{C}_s^{-1} \mathbf{X}_s)^{-1} \mathbf{X}_s' \mathbf{C}_s^{-1} \mathbf{y}_s$ is the general least-squares estimate of the system-specific coefficients. The remaining parameters were estimated by inserting results from Eq. (H-7) and Eq. (H-8) into Eq. (H-6) and using a simplex algorithm implemented in Matlab 7.2 (Mathworks, Natick, MA) to find the maximum likelihood.